Int. J. Heat Mass Transfer. Vol. 12, pp. 1553–1572. Pergamon Press 1969. Printed in Great Britain

RADIATION DOMINANT INTERACTION IN GASDYNAMICS†

KUEI-YUAN CHIEN‡
Massachusetts Institute of Technology, Aerophysics Laboratory, Cambridge, Massachusetts

(*Received* 24 *October* 1968 *and in revised form* 21 *April* 1969)

Abstract—The interaction between a dominant radiation field and a flow field is investigated, where the time scale for such an unsteady interaction may be quite short compared to a characteristic "flow" time. To lowest order there results a radiative cooling process with an uncoupled flow, and an expansion in Boltzmann number then systematically introduces higher order effects. A matched asymptotic expansion scheme is required in view of the disparate characteristic lengths that exist in different spatial regions. Results are presented for the specific example of instantaneous addition of energy to a finite region with one-dimensional symmetry (i.e. planar, cylindrical and spherical). For simplicity the gas is assumed inviscid, perfect and in local thermodynamic equilibrium, and the differential approximation is used for the radiative field. A numerical scheme was developed to avoid time consuming iterations and results are compared to those for an analytic solution limited to the linear case. Both nongrey approximations and up-stream absorption effects are included. Results indicate a negligible upstream heating level, moderate nongrey but large curvature and optical thickness effects. Depending on the local balance between emission and absorption, the blast shock can be either accelerated or decelerated. Finally, comparison between differential approximation and exact formulations for a planar grey case is made. Excellent agreement between the present work and a laser experiment indicates the possible energy coupling to be inferred.

NOMENCLATURE

a, isentropic speed of sound;
B_ν, Planck function;
Bo, Boltzmann number;
e, material specific internal energy;
G, mean radiative intensity;
I_ν, specific intensity;
$\mathbf{q}$, radiative flux vector;
T_0, core temperature;
T'_∞, ambient temperature;
T_∞, $\equiv T'_\infty/T_0$;
t_*, radiation "depletion" time;
$\mathbf{u}$, velocity vector;
w_i, quadrature weights;
x_∞, location where any radiative disturbance is negligible, equation (19);
α_{a_i}, moment weighted absorption coefficients for intensity, equations (9) and (10);
α_p, Planck mean absorption (emission) coefficient;
α_R, Rosseland mean absorption coefficient;
α_ν, volumetric absorption coefficient;
ζ, stretched time parameter, equation (36);
θ, similarity variable;
ν, photon frequency;
ξ, stretched spatial variable, equation (28);
ρ, material density;
τ, Bouguer number;
$( )^{(i)}$, ith order perturbation quantities;
$(\dot{})$, $\mathrm{d}/\mathrm{d}t$;
$(\tilde{})$, dimensionless variable;

† The author wishes to acknowledge the helpful discussions, advice and encouragement of Prof. J. R. Baron during the course of this investigation. He is also indebted to the other members of his thesis committee, Professors L. Trilling and J. L. Kerrebrock, for their constructive criticism. The work was sponsored by the U.S. Air Force, Office of Scientific Research under Contract No. AF49(638)-1621.

‡ Research Assistant, Aerophysics Laboratory, Department of Aeronautics and Astronautics.

$( )_c, ( )_s$, evaluated at contact surface, shock wave;
$( )_\nu$, spectral quantities;
$( )_*$, reference state.

INTRODUCTION

THE ROLE of thermal radiation in energy transport becomes increasingly significant in flows involving large gas temperatures. This study is specifically concerned with a case for which such radiative transport effects are dominant. In terms of the ratio of convective to black body radiative energy transfer, $(\rho uh/\sigma T^4)_{\text{ref.}}$ or Boltzmann number, such dominance implies $\text{Bo} \ll 1$. Such situations may arise, for example, due to the deposit of energy in a localized region from energy sources such as:

1. An explosion in the megaton range in air.
2. The focusing of a laser with a power output of hundreds of megawatts in air or other gases.
3. High altitude, high-speed flight of re-entry vehicles.

The possible importance of radiation is evident from the following example. An explosion of yield 20 kt of TNT may generate a temperature of $3 \times 10^5\,^\circ\text{K}$ in a 14 m spherical mass of air after about 10^{-4} s. The corresponding black body radiative power is $1{\cdot}13 \times 10^{28}$ ergs/s and in view of a total energy content of $8{\cdot}4 \times 10^{20}$ ergs implies a radiative "depletion" time of $7{\cdot}4 \times 10^{-5}$ sec.

Nevertheless, Taylor [2] correctly predicts the initial energy content of such blasts on the basis of a matching of the time history of the shock front to the experimentally observed luminous front for times larger than $\cong 2{\cdot}5 \times 10^{-4}$ s. On the other hand, a recent experiment in which ionization was induced by means of a pulsed laser beam was conducted by Daiber and Thompson [3] and indicated a luminous front location versus time behavior involving an exponent $N \simeq 0{\cdot}21$. This is in contrast to both the adiabatic [2, 4] and the radiation perturbed [5, 6] predictions of 0·4 or 0·5 for either spherical or cylindrical geometries.

Lall and Viskanta [7] previously considered the transient radiative cooling of such a spherical mass of gas under restrictions of both constant pressure at the boundary and absorption coefficient. Steady state problems with coupled and dominant radiation transport also have been considered by Lick [8], Wang [9] and Wang and Tien [10].

The special care required for dominant radiation situations is apparent from two methods recently extended to radiation gasdynamics. In the method of characteristics ([11] Sec. 6.2) there are difficulties associated with the characteristics study of large piston velocities (which generate very strongly radiating shock layers). Similarly, in the method of parametric differentiation [12], convergence proves to be increasingly difficult for stronger radiative transfer (see e.g. Fig. 9 of [12]). In both cases the problem is related to the singular behavior in the limit of a radiation dominated interaction.

Furthermore, the importance of the geometrical dilutation effect is not at all clear for the nonplanar case. Lastly, the time scale involved for the achievement of an appreciable upstream absorption level is of some interest. Thus the specific purposes for the present investigation may be stated as follows:

1. To construct a model suitable for the study of the interaction between dominant radiative transfer and a flowing fluid.
2. To study the effect of both geometry and gas model on the transient behavior of the flow field including upstream absorption effects.

GOVERNING EQUATIONS

Consider situations for which $T \sim 10^5$–$10^6\,^\circ\text{K}$ and densities comparable to that of sea level. It may be shown [13] that inviscid, nonconducting and nonscattering assumptions are reasonable, and that the time dependence term in the photon transfer equation is negligible. Under such conditions both the radiative

pressure and energy density remain small as compared to their material counterparts [13]. Therefore, the continuity, momentum and energy equation are the familiar forms,

$$\frac{D\rho}{Dt} + \rho\nabla.\mathbf{u} = 0 \tag{1}$$

$$\rho\frac{D\mathbf{u}}{Dt} + \nabla p = 0 \tag{2}$$

$$\rho\frac{De}{Dt} + p(\nabla.\mathbf{u}) + \nabla.\mathbf{q} = 0 \tag{3}$$

and are coupled to state and constitutive relations for the gas and the radiative transfer equation

$$\bar{\Omega}.\nabla I_\nu = \alpha_\nu(B_\nu - I_\nu) \tag{4}$$

required to specify the radiative flux $\mathbf{q}$

$$\mathbf{q} = \int_0^\infty \int_{4\pi} \bar{\Omega} I_\nu \, d\Omega \, d\nu. \tag{5}$$

Some additional simplifying assumptions will be made as follows:

1. The gas is both thermally and calorically perfect and in local thermodynamic equilibrium.
2. The radiant properties of the gas are characterized by a specification of *both* Planck and Rosseland mean absorption coefficients.
3. A differential approximation description of the radiative field is adopted (for a majority of the study) in place of the exact integral formulation; some checks with the latter will be indicated.

For equilibrium air $\gamma = 1{\cdot}33$ is a reasonable approximation for the conditions considered here [1], and the gas constant varies only by a factor of about two [13]. Assumption 2 is a suggested improvement over the grey gas model [14, 15]. Assumption 3 stems from curvature effects which imply multiple integrations (see e.g. [16]) and considerable mathematical complexity in an exact formulation. The differential approximation [17] offers considerable simplification and has been demonstrated to be both qualitatively correct and quantitatively of reasonable accuracy for certain cases [9, 11, 12, 16]. However this approximation may not be appropriate to use for problems involving nonplanar geometries with walls at different temperatures [29–31]. In the differential approximation the transfer equation (4) is replaced by two moment equations [15, 17]

$$\nabla.\mathbf{q} = 4\pi\alpha_p B - \alpha_{a_0} G \tag{6}$$

$$\nabla G = -3\alpha_{a_1}\mathbf{q} \tag{7}$$

where

$$G = \int_0^\infty \int_{4\pi} I_\nu \, d\Omega \, d\nu \tag{8}$$

is the mean radiative intensity and

$$\alpha_{a_0} = \frac{1}{G}\int_0^\infty \int_{4\pi} I_\nu \, d\Omega \, \alpha_\nu \, d\nu \tag{9}$$

$$\alpha_{a_1} = \frac{1}{q}\int_0^\infty \int_{4\pi} I_\nu \, \bar{\Omega} \, d\Omega \, \alpha_\nu \, d\nu \tag{10}$$

are intensity and flux averaged mean absorption coefficients, respectively [15]. Henceforth we shall refer to dimensionless variables, denoted by $\tilde{(\ )}$, relative to reference states, $(\ )_*$. For example, $\tilde{P} = P/P_*$ and all radiative properties are normalized by σT_* [4]. The reference velocity a_* is chosen to be the isentropic sound speed, R_* is a characteristic length, and the time t_* will be made specific later. For simplicity, the tilde notation will be suppressed from now on and all equations are to be understood as dimensionless.

From an order of magnitude analysis of the energy equation it follows that the appropriate time scale when $\mathrm{Bo} \ll 1$ is

$$t_* = \frac{\mathrm{Bo}}{(a_*/R_*)} = \mathrm{Bo}\, t_{\mathrm{flow}}, \text{ say} \tag{11}$$

which may be referred to as the (initial) radiation "depletion" time. A modification is required for

nonblack radiation, i.e. thin gases. In such instances the appropriate choice is

$$t_* = \frac{\mathrm{Bo}}{\tau(a_*/R_*)} = \frac{\mathrm{Bo}}{\tau} t_{\mathrm{flow}},$$

where $\tau = (\alpha_p R)_*$ is the Bouguer number, and $(\mathrm{Bo}/\tau) \ll 1$.

At sufficiently small times (i.e. $t_* \ll 1$), the rather uniform cooling process for a thin gas (in the "outer" region as discussed below) shows the present approach to be justified *a posteriori*. From equation (11) it follows that $t_* \ll t_{\mathrm{flow}}$ and thus the continuity and momentum equations imply that both $\partial\rho/\partial t$ and $\partial\bar{u}/\partial t$ are ~ 0 (Bo). Chow [18] took note of the $\partial\rho/\partial t$ behavior in the numerical work of Lall and Viskanta [7]. Physically, the implication is that unsteady dominant radiation interactions result primarily in a cooling process. Flow is induced by the radiation as higher order contributions through the nonhomogeneous cooling of the hot core. This suggests a systematic expansion in powers of Bo such as

$$f = f^{(0)} + \mathrm{Bo}\, f^{(1)} + 0(\mathrm{Bo}^2) \qquad (12)$$

where f represents any of the dependent variables. Quite general initial conditions can be used here to simulate various problems. However, without loss of generality, the initial conditions for $f^{(i)}$, $i \geqslant 1$, may be taken as homogeneous conditions.

It is of some interest to compare the several time scales involved and their magnitudes relative to t_*. For example, for 10^6 °K and sea level density, the thermalization time for ions and electrons is 10^{-9} s which is one order higher than the lifetime for atomic quantum transitions. The particle collision time is about 10^{-12} s. These may be compared with an (initial) radiation "depletion" time, t_*, of 4×10^{-7} s based on equilibrium air and R_* equivalent to a photon mean free path of about 1 m. It appears that such high temperature regions are collision dominated and close to equilibrium.

SPATIALLY ONE-DIMENSIONAL UNSTEADY EXAMPLES

To illustrate the basic ideas developed so far, let us consider the following simple model. A slab (or circular cylinder, or sphere of gas; i.e. a geometry with spatial symmetry) of semi-thickness (or radius) R_* at a uniform high temperature T_0 is assumed at $t = 0$. External to such a hot core there is an initially uniform region of temperature T'_∞. Normalizing relative to the initial core temperature, we have

$$T = \begin{cases} 1 \\ T'_\infty/T_0\,(\equiv T_\infty) \end{cases} \text{for} \quad x \lessgtr 1 \text{ at } t = 0. \qquad (13)$$

Implicitly such a hot core is generated with sufficient rapidity that the density remains uniform and the fluid motionless everywhere. For example, this may approximate the initial state of a "fireball" if the energy addition is completed in a time interval appreciably shorter than the characteristic flow time, $(R/a)_*$.

Utilizing the expansion procedure, equation (12), it follows that $\rho^{(0)} = 1$, $u^{(0)} = 0$ and the lowest order energy equation reduces to

$$\frac{\partial T^{(0)}}{\partial t} + \gamma\tau(4\alpha_p^{(0)} T^{(0)4} - \alpha_{a_0}^{(0)} G^{(0)}) = 0. \qquad (14)$$

The radiative field to the lowest order is governed by

$$\frac{1}{x^j}\frac{\partial}{\partial x}(x^j q^{(0)}) = \tau(4\alpha_p^{(0)} T^{(0)4} - \alpha_{a_0}^{(0)} G^{(0)}) \qquad (15)$$

$$\frac{\partial G^{(0)}}{\partial x} = -3\tau\alpha_{a_1}^{(0)} q^{(0)}. \qquad (16)$$

Here $j = 0$, 1 or 2 refers to planar, cylindrical or spherical geometries, respectively. $\alpha_p^{(0)} = \alpha_p(\rho^{(0)}, T^{(0)})$ and similarly for $\alpha_{a_0}^{(0)}$ and $\alpha_{a_1}^{(0)}$.

For the present model $\rho^{(1)}(x, t) = 0$; that is, the density remains constant after inclusion of first-order effects. The radiation induced flow field is governed by

$$\frac{\partial u^{(1)}}{\partial t} = -\frac{1}{\gamma}\frac{\partial T^{(0)}}{\partial x} \qquad (17)$$

with the initial conditions $u^{(1)} = 0$ and $T^{(0)}$ from equation (13). Symmetry dictates that $q^{(0)}(x = 0, t) = 0$. Finally, for thermodynamic equilibrium at $x \to \infty$,

$$T^{(0)} = T_\infty, \quad G^{(0)} = 4T_\infty^4, \quad q^{(0)} = 0. \quad \text{(18a, b, c)}$$

Optical properties have been based upon Traugott's harmonic mean model [19] for α_p, and $\alpha_R = 0{\cdot}3\ \alpha_p$ as suggested in Table 5·2 of [1]. It is realized that such a representation for α_R is inappropriate at low temperatures ($T < 1$ eV).

Three gas models have been employed in order to indicate possible spectral effects: grey (with mean absorption coefficient α_p), semigrey [15] and Traugott's [14]. The latter two models provide some improvement in the representation at least in the thick gas limit. Finkleman and Chien [15] have shown Traugott's model [14] to be incorrect near radiative equilibrium. However, the utility of a quasi-isotropy assumption [15] (i.e. $\alpha_{a_0} = \alpha_{a_1}$) has not been documented.† Thus all of the results to be displayed must be considered as qualitative, whereas the method itself is not restricted to specific absorption models.

Finally, it is to be noted that the characteristics of equations (14) and (17) are orthogonal to those of equations (15) and (16). Thus equation (14) may be integrated in t along x = constant, and for each incremental time equations (15) and (16) can similarly be integrated in x. In practice $x \to \infty$ may be replaced by some $x_\infty \gg 1$, corresponding to the location where radiative disturbances are negligible. In essence this implies the approximation

$$T^{(0)} \sim T_\infty \qquad \text{for} \quad x \geqslant x_\infty \qquad (19)$$

which is physically reasonable if x_∞ is chosen to be several photon mean free paths distant from the interface ($x = 1$). In view of the anticipated exponential decay of the radiation field, x_∞ has arbitrarily been chosen to be 5 photon mean free paths (based on T_∞) away. Consistent with this is the condition on the radiative properties of $q^{(0)}$ and $G^{(0)}$. For such a near uniform temperature distribution, in combination with the equilibrium condition at $x \to \infty$, equations (18b, c) the radiation field is described by [11]

$$G^{(0)}(x_\infty) = 4T_\infty^4 + g_j q^{(0)}(x_\infty) \sqrt{\left(\frac{3\alpha_{a_1}(T_\infty)}{\alpha_{a_0}(T_\infty)}\right)} \qquad (20)$$

where

$$g_j = \begin{cases} 1 \\ K_0(\eta_1)/K_1(\eta_1) \\ \eta_1(\eta_1 + 1) \end{cases} \quad \text{for} \quad j = \begin{cases} 0 \\ 1 \\ 2 \end{cases} \qquad (21)$$

K_0 and K_1 are modified Bessel's functions, and

$$\eta_1 = \tau x_\infty \sqrt{[3\alpha_{a_0}(T_\infty)\, \alpha_{a_1}(T_\infty)]}. \qquad (22)$$

For a grey gas and a plane geometry, equation (20) simply reduces to the boundary condition derived by Cheng [20].† Physically, a planar, uniform gas of infinite thickness corresponds to a black body radiating at the gas temperature T_∞. Consistent with the differential approximation, the black body condition corresponds to equation (20) for $j = 0$. However, equation (21) also includes curvature effects and a representation of the nongrey behavior of the gas. For $\eta_1 \gg 1$, i.e. large x_∞, both the cylindrical and spherical cases behave essentially planar as would be anticipated. Moreover, both the grey and semigrey [15] (but not Traugott's [14, 15]) gas models imply $\alpha_{a_0} = \alpha_{a_1} = \alpha_p$ at $T = T_\infty$ as required for radiative equilibrium.

Clearly the imposed two-point boundary value problem requires time-consuming iteration at each time increment. Moreover the conditions for $x \gg 1$ imply a saddle point as noted by Sherman [21] and Finkleman [11]. Such difficulties can be avoided upon recasting the problem into dual integral equations prior to numerical manipulations, and without restriction to the present expansion procedures [13].

† For some simple problems evidence exists that all three mean absorption and emission (Planck) coefficients can behave quite differently [32, 33].

† With the exception that the factor $\sqrt{3}$ in equation (20) is replaced by 2 (see [11] also).

The method starts from the differential approximation for spatially one-dimensional problems [e.g. equations (15) and (16)], which can be written alternatively as

$$x^j q(x,t) = \tau \int_{\gamma_0}^{x} y^j (4\alpha_p T^4 - \alpha_{a_0} G)\,\mathrm{d}y + x_0^j q(x_0,t) \qquad (23)$$

$$G(x,t) = G(x_0',t) - 3\tau \int_{x_0'}^{x} \alpha_{a_1} q\,\mathrm{d}y \qquad (24)$$

x_0 and x_0' being arbitrary locations. Utilizing quadrature approximations for the integrals, such as

$$\int_a^b f(x)\,\mathrm{d}x \cong \sum_{i=1}^{N} W_i f(x_i) \qquad (25)$$

for N points in the interval $(0, x)$ there results from equations (23)–(25), $2N - 2$ linear algebraic equations for $2N$ unknowns. Another condition is imposed by the symmetry requirement, $q(0,t) = 0$. The last relation follows from equation (20). Standard matrix inversion techniques now furnish the solution for the radiation field.

Several points should be noted. First, since the original dual integral equations are of the Volterra type, a quadrature with uniform increments proves to be much easier to apply barring use of the crudest trapezoidal rule throughout. Secondly, since the accuracy of the quadrature formula generally depends on higher order derivatives of the integrand in the range under consideration, problems involving a discontinuity (e.g. the model used here or in any flows with shock waves) at $x = 1$, say, may be split into two parts: the intervals $0 \leqslant x \leqslant 1$ and $1 \leqslant x \leqslant x_\infty$. Within each interval the

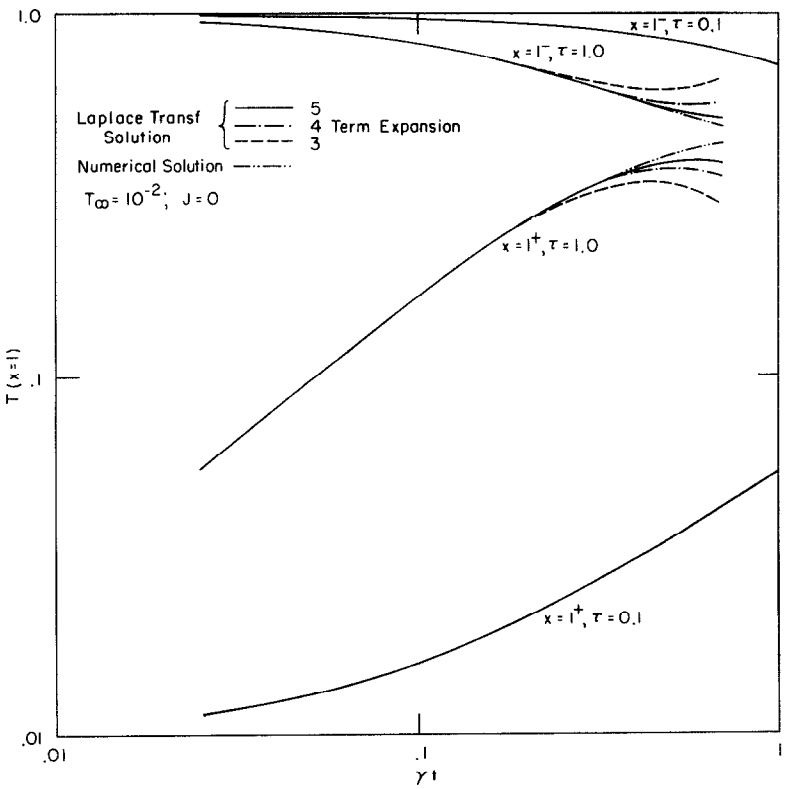

FIG. 1. Comparison of interface temperature variations according to several methods.

reduction from dual integral equations to simultaneous linear algebraic equations may be applied separately. Two additional boundary (matching) conditions then follow from the continuity of G and q at $x = 1$. Finally, the reference points x and x_0' in equations (23) and (24) may be chosen so as to include a maximum number of points between the reference and field points, so as to improve quadrature accuracy.

A linear model† has been used to check on both the numerical scheme and the far field assumption, equation (19). Analytic solutions were obtained using the Laplace transform technique for small times [13]. It is seen (Fig. 1) that numerical results do converge to the analytic solutions within the latter's range of validity. Furthermore, the far field approximation [equations (19)–(21)] does not appreciably effect the solution near $x = 1$.

Encouraged by the results obtained for the linear problem, we may now embark on nonlinear cases. However, it must be noted that the regular expansion procedure employed thus far will not be valid everywhere due to the disparate characteristic lengths existing in different regions of the problem, as considered next.

INNER EXPANSION PROCEDURE

The above representation with flow induced due to nonuniform radiative cooling is not uniformly valid if sharp gradients exist initially at the boundary of the hot gas region, i.e. "close" to the interface, the proper characteristic length is the local distance from the interface in contrast to the overall dimension of the hot region R_*. The local "flow" time, t_l, near an interface, $x = 1$, is

$$t_l = |x - 1|\frac{R_*}{a_*} = |x - 1|\frac{t_*}{\mathrm{Bo}}. \tag{26}$$

† Setting $\alpha_p = T^{-3}$ and $\alpha_{a_0} = \alpha_{a_1} = 1$.

Hence when

$$x = 1 + 0(\mathrm{Bo}) \tag{27}$$

t_l and t_* will be of identical order, and this occurs in a region of nonuniformity which is very small.

Consequently, close to the interface we are led to introduce a new (stretched) spatial variable

$$\xi = [x - x_s(t)]/\mathrm{Bo} \tag{28}$$

where $x_s(t)$ is the (foreseen) trajectory of a (shock) discontinuity imbedded inside the inner region. Within the framework of $t_l = t_* \ll (R_*/a_*)$

$$x_s(t) = 1 + \mathrm{Bo}\, x_{s_1}(t) + 0(\mathrm{Bo}^2) \tag{29}$$

and thus equation (28) implies $|\xi| \sim 0(1)$ in accordance with equation (27). After transforming from an (x, t) to a (ξ, t) description, we may again expand the dependent variables in powers of Bo as in equation (12).

Consider now the initial conditions. At $t = 0$, the entire inner region collapses into the single point $x = 1$. This suggests a conical solution near $t = 0$, and hence the utility of introducing

$$\theta = \xi/t. \tag{30}$$

The final form of the lowest order governing equations written in their characteristic forms are now (omitting the superscript zero for simplicity):

Along

$$\frac{\mathrm{d}\theta}{\mathrm{d}t} = \frac{u - \dot{x}_{s_1} - \theta}{t}; \tag{31}$$

$$-(\gamma - 1)\frac{T}{\rho}\frac{\mathrm{d}\rho}{\mathrm{d}t} + \frac{\mathrm{d}T}{\mathrm{d}t} = -\frac{\gamma\tau}{\rho}(4\alpha_p T^4 - \alpha_{a_0} G). \tag{32}$$

Along

$$\frac{\mathrm{d}\theta}{\mathrm{d}t} = \frac{u - \dot{x}_{s_1} - \theta \pm \sqrt{T}}{t} \tag{33a, b}$$

$$\pm \frac{\sqrt{T}}{\gamma\rho}\frac{d\rho}{dt} + \frac{du}{dt} \pm \frac{1}{\gamma\sqrt{T}}\frac{dT}{dt}$$

$$\pm \frac{\tau}{\rho\sqrt{T}}(4\alpha_p T^4 - \alpha_{a_0} G) = 0 \qquad (34a, b)$$

$$\frac{\partial q}{\partial\theta} = \frac{\partial G}{\partial\theta} = 0 \qquad (35)$$

Thus the radiation field is not attenuated within this region. Simply, to this order the inner solution represents a flow with local heat addition (subtraction). The global dependence part of the radiation field, G, is prescribed solely by the outer solution. Thus with G uniform across the inner region and determined by the outer problem for all time. the governing equations (31)–(34b) may b\ solved by the method of characteristics.

However, in view of the complexity of the flow some method to render the problem tractable analytically is preferable to a strict application of the method of characteristics.

It can be shown [13] that for $t \ll 1$ the radiation effects are relatively small. Physically, the picture is that of a conical flow perturbed by radiation for such small times. Let us introduce the isentropic speed of sound $a \equiv \sqrt{T}$ and consider a time perturbation $t \sim 0(\varepsilon)$ where $\varepsilon \ll 1$. Introduce also a "stretched" time

$$\zeta = t/\varepsilon \qquad (36)$$

such that $\zeta \sim 0(1)$. Now consider an expansion of the dependent variables

$$f = f^{(0)}(\theta, \zeta) + \varepsilon f^{(1)}(\theta, \zeta) + 0(\varepsilon^2) \qquad (37)$$

where f represents ρ, u or a. Similarly, both the shock and the contact surface velocity expressions are expanded as

$$\dot{x}_{s_1}(t) = \dot{x}_s^{(0)} + \varepsilon\zeta\dot{x}_s^{(1)} \qquad (38)$$

$$\dot{x}_{c_1}(t) = \dot{x}_c^{(0)} + \varepsilon\zeta\dot{x}_c^{(1)}. \qquad (39)$$

Here the $\dot{x}_c^{(i)}$ and $\dot{x}_s^{(i)}$ $(i = 0, 1)$ are constants to be determined from equations (31)–(34) and $\dot{x}_{s_1}(t)$ and $\dot{x}_{c_1}(t)$ are obtained by differentiation from the positions of the shock and the contact surface

$$x_s(t) = 1 + \mathrm{Bo}\, x_{s_1}(t) \qquad (40)$$

$$x_c(t) = 1 + \mathrm{Bo}\, x_{c_1}(t). \qquad (41)$$

Substituting equations (37)–(39) into (31)–(34b) and equating terms of identical powers in ε, results to the lowest order in the classical solution of a planar adiabatic shock tube. The shock velocity $\dot{x}_s^{(0)}$ is governed by

$$T_\infty = \left\{1 + \frac{2\gamma}{\gamma+1}\left(\frac{\dot{x}_s^{(0)2} - T_\infty}{T_\infty}\right)\right\} \times \left\{1 - \frac{\gamma-1}{\gamma+1}\left(\frac{\dot{x}_s^{(0)2} - T_\infty}{\dot{x}_s^{(0)}}\right)\right\}^{2\gamma/(\gamma+1)} \qquad (42)$$

which may be solved numerically, for example, by Newton's method of successive approximations.

To the next order, we obtain

$$\frac{d\zeta}{\zeta} = \frac{d\theta}{u^{(0)} - \dot{x}_s^{(0)} - \theta} = \frac{(1-\gamma)\dfrac{a^{(0)}}{\rho^{(0)}}d\rho^{(1)} + 2da^{(1)}}{f^{(1)}} \qquad (43)$$

$$\frac{d\zeta}{\zeta} = \frac{d\theta}{a^{(0)} - \dot{x}_s^{(0)} - \theta \pm a^{(0)}} = \frac{\pm\dfrac{a^{(0)}}{\gamma\rho^{(0)}}d\rho^{(1)} + du^{(1)} \pm \dfrac{2}{\gamma}da^{(1)}}{f_\pm^{(2)}} \qquad (44)$$

where

$$f^{(1)} = (\gamma-1)\frac{d\rho^{(0)}}{d\theta}\left\{\frac{a^{(0)}}{\rho^{(0)}}[u^{(1)} - \dot{x}_s^{(1)}\zeta] + \frac{a^{(1)}}{\rho^{(0)}} - \frac{a^{(0)}\rho^{(1)}}{\rho^{(0)2}}(u^{(0)} - \dot{x}_s^{(0)} - \theta)\right\} - 2[u^{(1)} - \dot{x}_s^{(1)}\zeta]\frac{da^{(0)}}{d\theta} - \frac{\zeta\gamma\tau}{\rho^{(0)}a^{(0)}} \times [4\alpha_p^{(0)}a^{(0)8} - \alpha_{a_0}^{(0)}G]$$

and

$$f_{\pm}^{(2)} = \mp \frac{1}{\gamma}\frac{d\rho^{(0)}}{d\theta}\left\{\frac{a^{(0)}}{\rho^{(0)}}[u^{(1)} - \dot{x}_s^{(1)}\zeta + a^{(0)}] + \left[\frac{a^{(1)}}{\rho^{(0)}} - \frac{a^{(0)}\rho^{(1)}}{\rho^{(0)2}}\right] \times (u^{(0)} - \dot{x}_s^{(0)} - \theta \pm a^{(0)})\right\} - \{u^{(1)} - \dot{x}_s^{(1)}\zeta \pm a^{(1)}\}\frac{d}{d\theta}\left[u^{(0)} \pm \frac{2a^{(0)}}{\gamma}\right] \mp \frac{\zeta\tau}{\rho^{(0)}a^{(0)}}\{4\alpha_p^{(0)}a^{(0)^4} - \alpha_{a_0}^{(0)}G\}.$$

The characteristic directions are determined by the zeroth order quantities. As a result, within the time scale $\xi \sim 0(1)$, the discontinuity in slope at the tail of the expansion fan (θ_{ET}) does not develop into a shock wave. A similar conclusion for the radiation-free case has been found by McFadden [22]: no secondary shock originates at θ_{ET} in a nonplanar geometry. This is clearly invalid for $\zeta \sim 0\ (1/\varepsilon)$ [23, 24] which has not been considered here.

In view of the simple (uniform) base solutions everywhere except in the expansion region, closed form solutions are obtained by the characteristics method. Crudest numerical approximation (without iteration) has been used in the expansion region. The detailed form of the solutions are included in [13].

RESULTS AND DISCUSSION

Five major parameters characterize the problem, namely γ (= 1·33 here), τ, j, the ratio of the ambient to the initial core temperature, and a

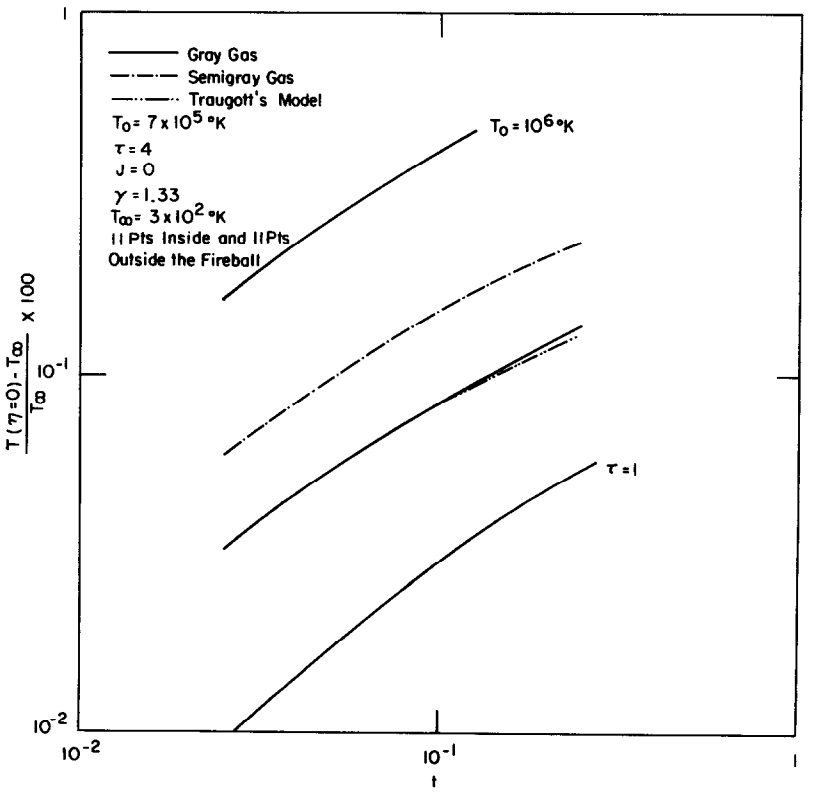

FIG. 2. Effects of Bouguer number, core temperature and gas model on the interface upstream heating level (planar cases).

characteristic describing the gas model. Since a fixed ambient temperature (300°K) was used, variations in the ratio of the ambient to the initial core temperature indicate changes in the latter, which in turn affects the Boltzmann number and the characteristic time t_*.

Shown in Fig. 2 is the precursor heating effect on the gas immediately upstream of the interface for a planar case. Due to the absence of a curvature effect, the planar case serves as an upper bound on the upstream heating level for all three geometries considered. It is clear that the effect of nongreyness, Bouguer number and core temperature are considerable but the overall upstream heating effect remains negligible. Therefore, within the time scale associated with a radiation dominant interaction the assumption of a uniform upstream temperature does indeed appear to be a reasonable approximation. Some caution must be exercised since this slow initial upstream heating rate may eventually change due to the nonlinear dependence uf α_p on T. Nevertheless, this does supply further justification for the strong shock approximation employed by Taylor [2].

Figure 3 displays the distributions of the heat flux in time. It is clear that nonplanar cases possess shorter characteristic times than does the planar case, consistent with intuition based upon the larger ratio of surface area to volume for the former. Note that q for $j = 1$ is the largest. However, since the ratio of surface area to volume is equal to $(j + 1)$ per unit radius (semi-thickness), the energy left in the core will decrease most rapidly for $j = 2$, as one might expect (see below).

In Fig. 4 are shown the effects on the radiative flux q at the interface $x = 1$. Due to the stronger

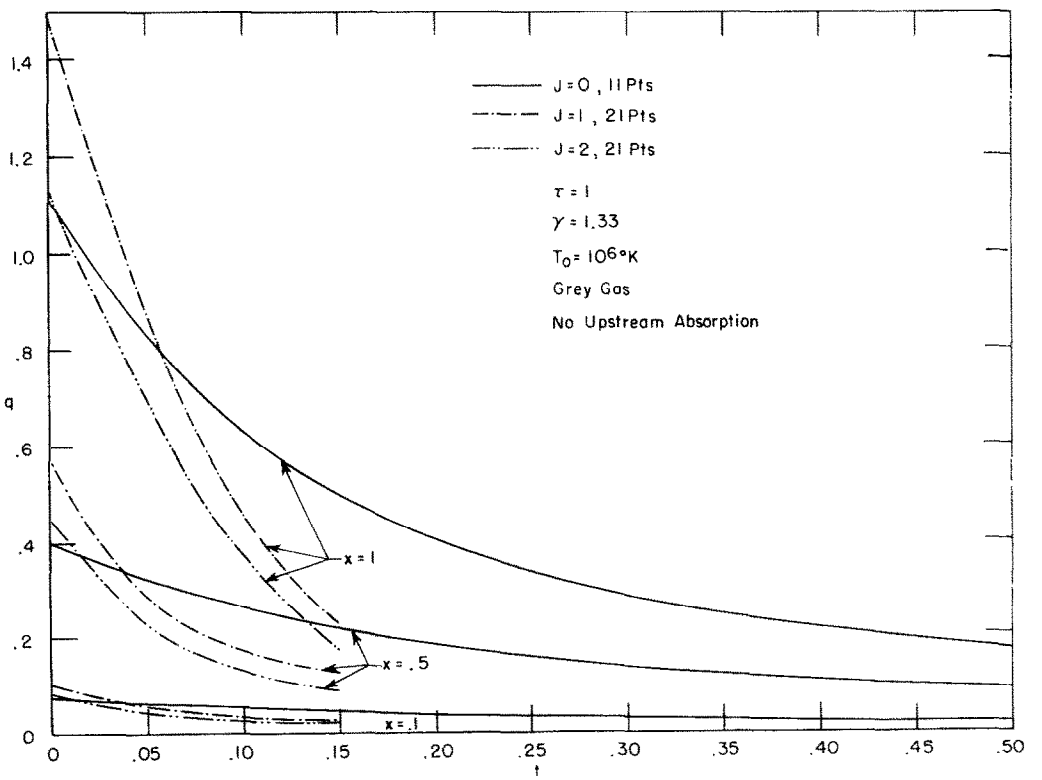

FIG. 3. Geometrical effect on heat flux at $\tau = 1$.

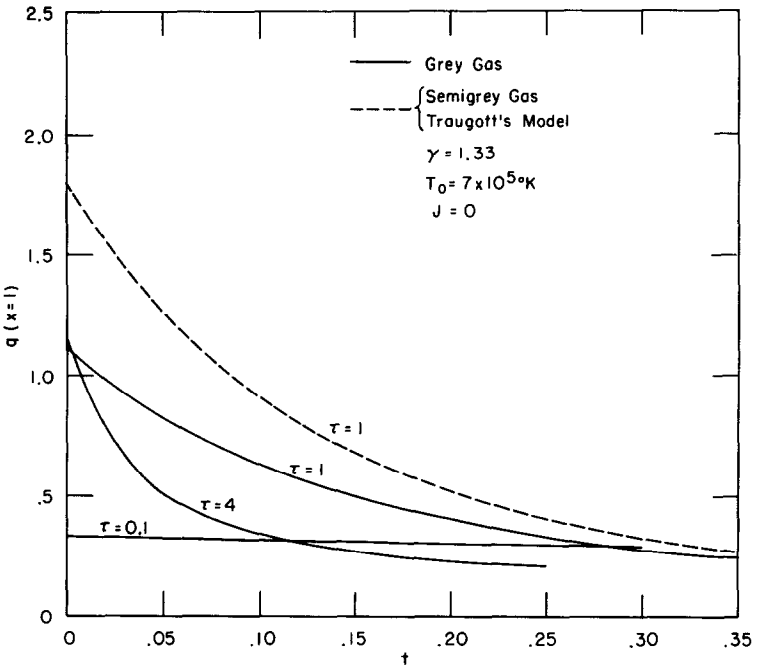

FIG. 4. Effect of Bouguer number and nongrey gas model on the temporal behavior of the interface heat flux.

interior blocking effect for an optically thicker gas (larger τ), only a thin layer of thickness $\sim 0(1/\tau)$ near the interface is cooled significantly. This results in a shorter characteristic time than those applicable for smaller τ. For $\tau \ll 1$, the entire volume participates in the cooling process but the rate of cooling is quite small. Furthermore, for the absorption coefficients model used here, both nongrey representations give practically the same temporal behavior of the heat flux. For $\tau = 1$ it is seen that allowance for nongreyness implies stronger radiation, but the qualitative trend remains the same.

Figures 5 and 6 depict the radiation induced velocity for different gas models and geometries. In our model $u = \mathrm{Bo}\,.\,u^{(1)}$. Due to a rather negligible upstream heating, $u^{(1)}$ proves to be independent of the core temperature (i.e. Bo), and as a result of the less uniform cooling proves to be larger for optically thick and nonplanar cases. The apparent nongrey effect again proves to behave qualitatively in quite the same way as the grey.

Of some interest is the energy E denoting the percentage of energy left in the core

$$E = (j+1)\int_0^1 T x^j \,\mathrm{d}x = 1 - \gamma(j+1)\int_0^t q(1,t)\,\mathrm{d}t \qquad (45)$$

the latter following from the energy equation, and physically simply expressing the initial energy minus that radiated away. From Fig. 7 it is clear that:

1. For an optically thin gas, E is virtually linear in t as a result of the slow rate of change of $q(1, t)$ (Fig. 4).

2. Because of the lesser blocking effect, E decreases to lower levels for nonplanar cases.

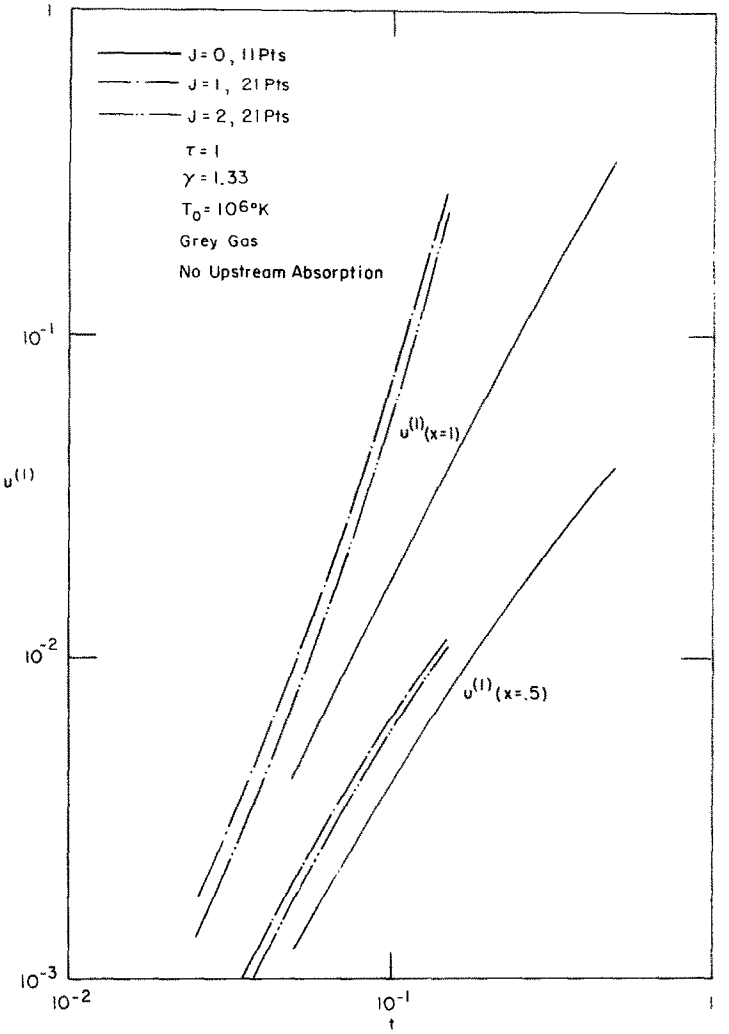

FIG. 5. Geometrical effect on the radiation induced velocity at $\tau = 1$.

3. Two numerical approximations, utilizing either 11 or 21 points inside the hot gas core, give good agreement with one another and furnish some indication of the reliability of the method.

4. Due to the negligible upstream heating (Fig. 2) the precursor effects have little influence on the prediction of E.

5. At a fixed t, as τ increases initially from small to intermediate values, E drops to a lower level because of the stronger emission effect. However, with increasing thickness the interior blocking confines the cooling process to a thin layer $\sim 0(1/\tau)$ near the interface, and the final E "asymptote" is above the minimum.

Figure 8 depicts again the curvature effect at $\tau = 1$, which is more pronounced than for $\tau = 0{\cdot}1$ (Fig. 7). The higher flux for a nongrey gas implies lesser E values.

Recall that the inner problem consists of a similarity solution of the shock tube type perturbed by radiation. For air at $T = 7 \times 10^5$

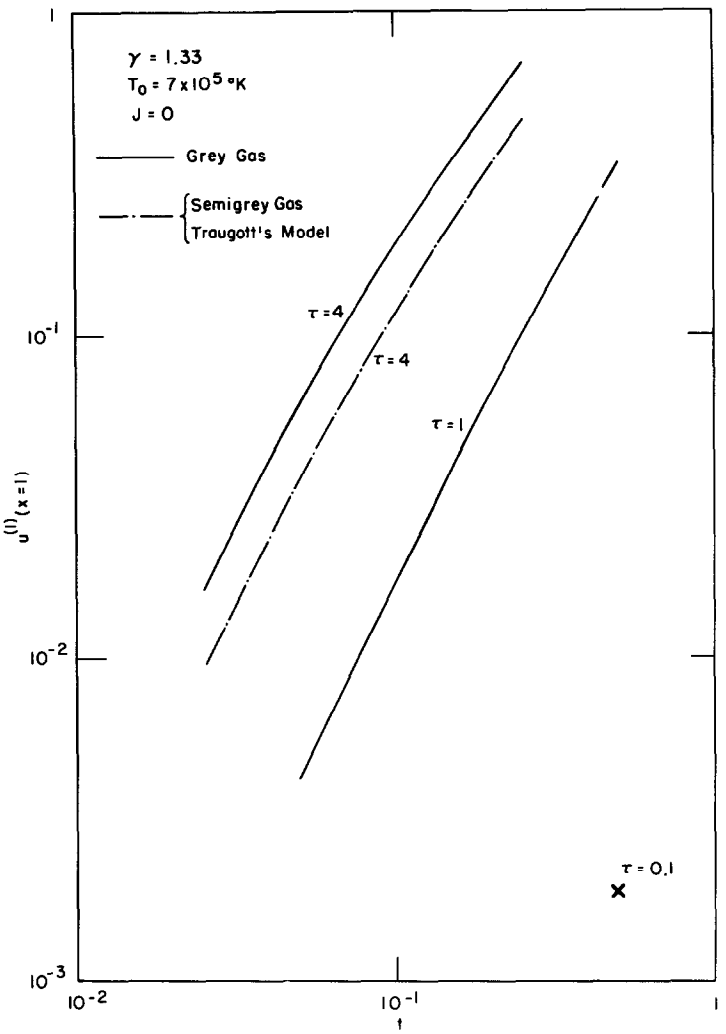

FIG. 6. The radiation induced velocity at the interface: Bouguer number and gas model effects.

and 10^6 °K, $\dot{x}_s^{(0)} = 0{\cdot}639$ and $\dot{x}_c^{(0)} = 0{\cdot}548$ while $\dot{x}_c^{(1)}$ and $\dot{x}_s^{(1)}$ can be of either sign. Figure 9 shows the effect of radiation on the pressure profile. For $\tau = 2$ ($j = 1$), the shock layer is sufficiently thick to absorb more energy than is emitted away. For $\tau = 0{\cdot}5$ ($j = 1$ or 2), on the other hand, the shock layer is sufficiently thin that emission dominates. The result is a pressure increase (decrease) in the shock layer for the thicker (thinner) case. Due to the lower ability to absorb radiation when $j = 2$, the pressure drop is greater. Within the expansion fan the pressure decreases with time due to the continual loss of energy but due to the much higher temperature levels of the "driver" gas the drop for both cylindrical and spherical cases proves to be almost identical. Since the thin layer is far from radiative equilibrium, the thicker gas involves a larger pressure drop. Due to energy addition (removal), the shock layer actually expands (contracts). There results an accelerating (declerating) shock wave while

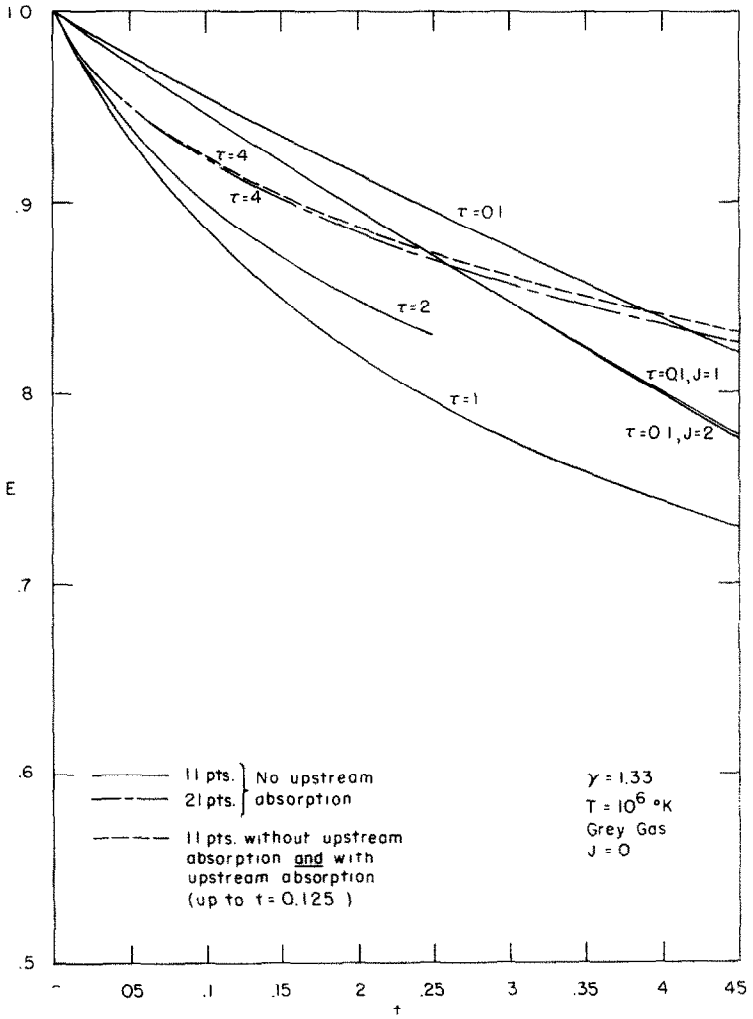

FIG. 7. The temporal behavior of core energy for several Bouguer numbers, geometries and numerical schemes.

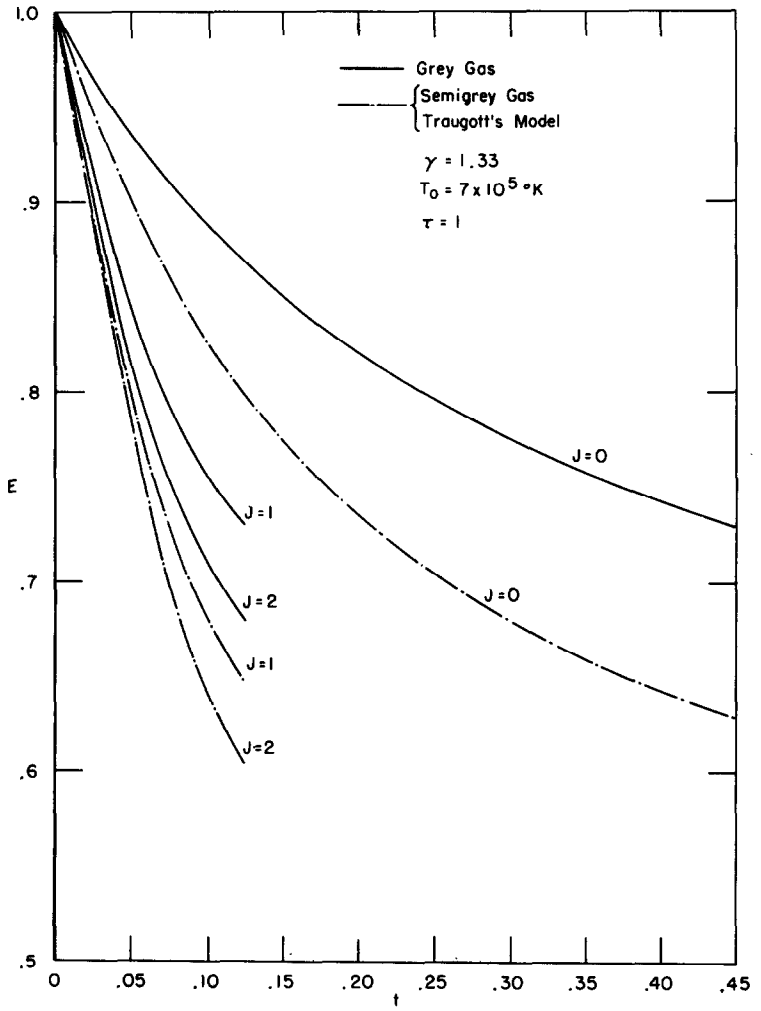

FIG. 8. Nongrey and geometrical effect on core energy.

simultaneously the contact surface is retarded (accelerated). A similar situation has been noted by Magee and Hirschfelder [25] in that the blast (shock) wave is strengthened due to the presence of NO_2 (strong radiation absorbing gas) near the periphery at the later stage of an explosion ($t \sim 10^{-2}$ s).

A comparison of $\dot{x}_s^{(1)}$ as predicted by both the differential approximation and an exact solution for the planar, grey case is presented in Fig. 10, and shows the ratio to be about 0·4 at $\tau = 10^{-2}$. Since it is the absorption term that is approximated by means of the differential approximation, the difference between the approximate and the exact formulations is expected to be small when close to emission dominance. Due to the rather low shock layer temperature (as compared to the driver gas) obtained from the shock tube solution (0·0664), the shock layer is emission dominated only for $\tau \gtrsim 10^{-7}$ and the ratio of $\dot{x}_s^{(1)}$ predicted by the two methods does approach unity at such low values. However, the continuum approach may be justified only for $\tau \geqslant 10^{-2}$. For $\tau \geqslant 10^{-2}$ ($j = 0$) the shock layer is locally absorbing more energy (from the much hotter driver gas)

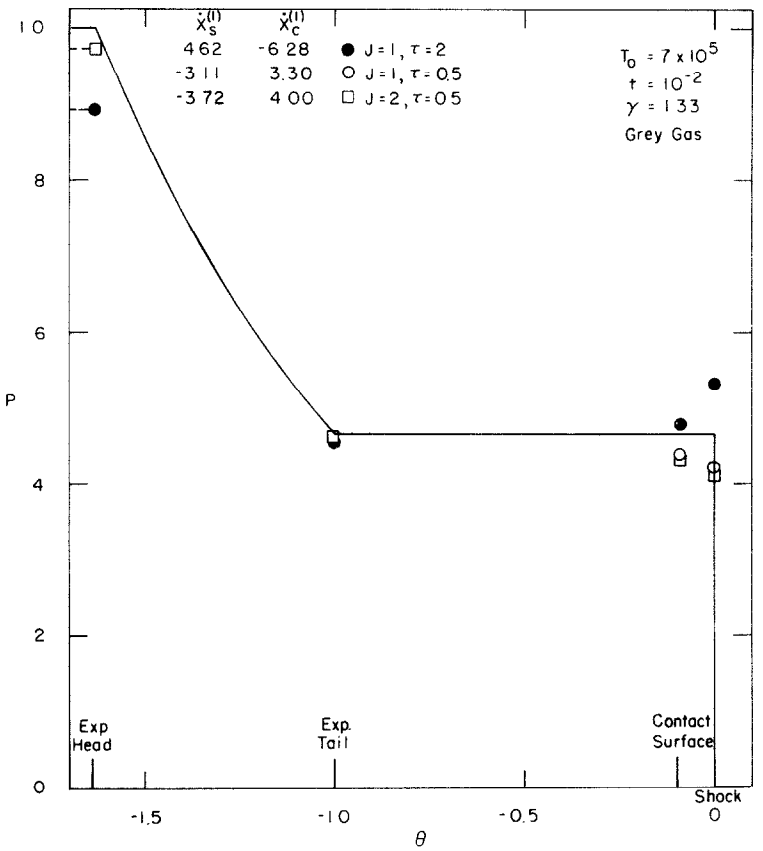

FIG. 9. Pressure distribution in the inner region: Geometric and Bouguer number effects.

than is being emitted away. Thus this is essentially a comparison of the mean intensity G. Overall, then a discrepancy of about two exists towards the optically thin end, and a vanishingly small error for $\tau \geqslant 1$. Similar conclusions have been reported by Kulander [26].

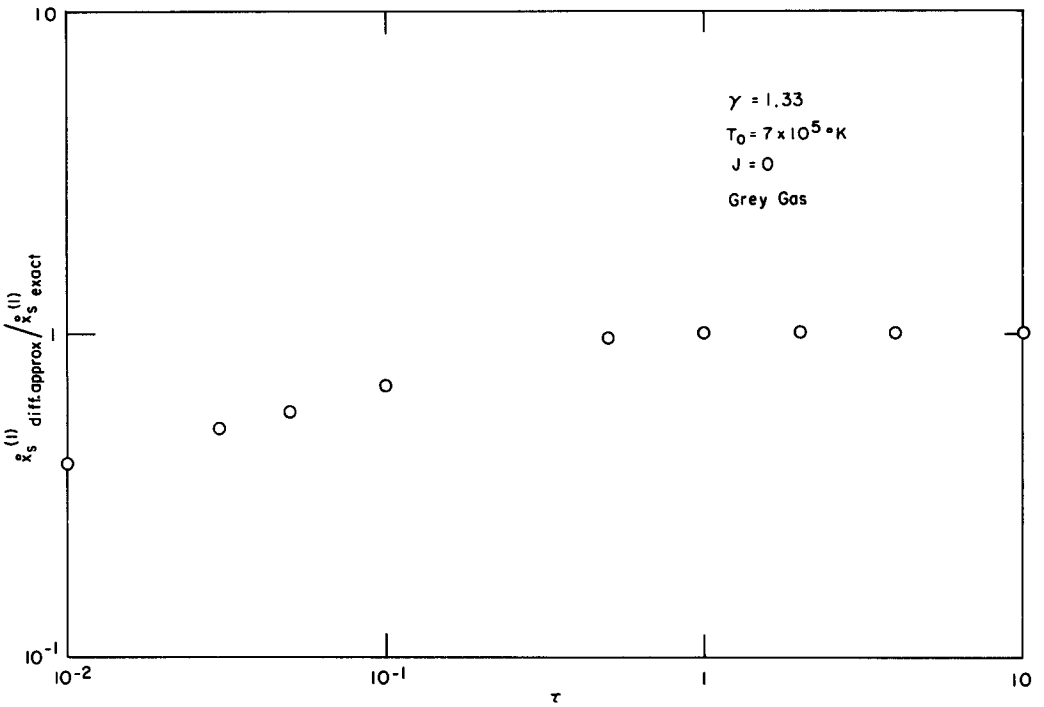

FIG. 10. Comparison of differential approximation and exact solution results for the radiation induced shock wave acceleration (planar case, grey gas).

CONCLUDING REMARKS

We may consider the physical phenomena responsible for the earlier observed results mentioned in the introduction. As shown earlier (Fig. 2), the extrapolated upstream heating level for the present time scale is negligible when compared to that of the hot core. Furthermore, for the experimental example considered by Taylor in his blast wave analysis, the gas proves to be optically thick ($\tau \sim 10^3$). Thus it is the strong blocking effect in the interior of the core which results in a negligible energy loss and permits similarity to be assumed.

On the other hand, in the experiment conducted by Daiber and Thompson [3] the gas was optically thin; for such an emission dominated ionized gas region a considerable amount of energy is lost by radiation and similarity fails. A detailed evaluation of the properties within such an ionized region immediately after the laser cut-off is beyond the present analysis. However, we may estimate the *mean* properties existing in such a "blob" of hot gas. Iteration (equilibrium air, $\gamma = 1{\cdot}33$) results in a hot core temperature of $\sim 6{\cdot}5 \times 10^5$ °K based on the radiation supported detonation wave theory proposed originally by Ramsden and Savic [27] (see also [1], Chapter 5). Alternatively, a constant volume heating model results in a mean temperature of

$6{\cdot}5 \times 10^5$ °K. The agreement is viewed as some evidence for the formation of a "fireball" due to the optical breakdown of air. A similar discovery of a "fireball' behavior existing in a laser product micro-explosion has also been found by Askaryan *et al.* [28].

If the location of the luminous fronts at the laser-off time t_0 is x_0, then experimental correlation [3] gives $(x/x_0) = (t/t_0)^N$ with $N = 0{\cdot}21$. For times sufficiently near t_0, for which the present radiation perturbed inner solution is valid, this can be expanded to allow a direct comparison with the shock wave trajectory, i.e.

$$\dot{x}_s^{(0)} = \frac{N}{\mathrm{Bo}} \frac{t_*}{t_0} \tag{46}$$

$$\dot{x}_s^{(1)} = \frac{N(N-1)}{\mathrm{Bo}} \left(\frac{t_*}{t_0}\right)^2 \tag{47}$$

From the definition of t_*, equation (11), and identification of x_0 with R_*, we obtain

$$\dot{x}_s^{(0)} = N\left(\frac{R_*}{a_* t_0}\right) \tag{48}$$

$$\dot{x}_s^{(1)} = N(N-1)\,\mathrm{Bo}\left(\frac{R_*}{a_* t_0}\right)^2 \tag{49}$$

Clearly in the above relations, R_* and t_0 are experimentally determined, whereas a_* and Bo are calculated from the experimental conditions. To generalize the calculation, we make use of the radiation supported detonation wave theory, in which, R_*/t_0 is related to the velocity of the "shock" at t_0, D_0, by $R_*/t_0 = c_1 D_0$ where $c_1 = 1{\cdot}67$. Furthermore, since the theory implies $D_0/a_* = (\gamma + 1)/\gamma$, then

$$\dot{x}_s^{(0)} = c_1\left(\frac{\gamma+1}{\gamma}\right)N \tag{50}$$

$$\dot{x}_s^{(1)} = c_1^2 N(N-1)\,\mathrm{Bo}\left(\frac{\gamma+1}{\gamma}\right)^2 \tag{51}$$

With $N = 0{\cdot}21$, $T_0 = 7 \times 10^5$ °K and $\gamma = 1{\cdot}33$, the experimentally observed values are $\dot{x}_s^{(0)} = 0{\cdot}61$ and $\dot{x}_s^{(1)} = -0{\cdot}087$†, which may be compared with the "shock tube" theory result, $\dot{x}_s^{(0)} = 0{\cdot}64$. From the harmonic model [19] for α_p, $R \sim 0{\cdot}4$ cm corresponds to $\tau \sim 3 \times 10^{-3}$ and results in $\dot{x}_s^{(1)} = -0{\cdot}023$. However, the harmonic model differs from the available data by anywhere from three to one orders of magnitude. For $\tau = 3 \times 10^{-2}$: $\dot{x}_s^{(1)} = -0{\cdot}23$; and for $\tau = 10^{-2}$: $\dot{x}_s^{(1)} = -0{\cdot}075$. The above calculations are for $j = 1$ and 2 and virtually all gas models. Note that for nonplanar geometries, $G(1, t) \ll 1$ follows from equations (20) and (21), which utilizes the equilibrium condition at $x \to \infty$, equations (18b, c).

In view of the asymmetries existing in the experiment, consideration of a reduction of R_* by a factor of one-half brings the upper bound to $\tau = 1{\cdot}5 \times 10^{-2}$, corresponding to $\dot{x}_s^{(1)} = -0{\cdot}11$.

In view of uncertainties in the "initial" conditions at $t = t_0$ as well as assumptions made herein, the experiment of Daiber and Thompson appears consistent with the present model taking $\tau \sim 10^{-2}$. Physically, due to the extremely low ability to absorb radiation, the shock layer is cooled by the local (dominant) emission process and results in a decelerating shock wave

REFERENCES

1. Ya. B. Zeldovich and Yu. P. Raizer, *Physics of Shock Waves and High Temperature Hydrodynamic Phenomena* Academic Press, New York (1966).
2. G. I. Taylor, The formation of a blast wave by a very intense explosion, *Proc. R. Soc.* **A201**, 159–186 (1950).
3. J. W. Daiber and H. M. Thompson, Laser-driven detonation waves in gases, *Physics Fluids* **10**, 1162–1169 (1967).
4. L. I. Sedov, *Similarity and Dimensional Methods in Mechanics*. Academic Press, New York (1959).
5. R. A. Gross, Continuum radiation behind a blast wave, *Physics Fluids* **7**, 1078–1080 (1964).
6. L. A. Elliott, Similarity methods in radiation and hydrodynamics, *Proc. R. Soc.* **A258**, 287–301 (1960).
7. P. S. Lall and R. Viskanta, Transient energy transfer in a grey radiating gas during expansion, *Physics Fluids* **10**, 98–107 (1967).

† If direct substitution of the values reported in [3] are used (i.e. $R_* \sim 0{\cdot}4$ cm and $t_0 \sim 25$ n s) in equations (48) and (49), then $\dot{x}_{s_{\mathrm{exp}}}^{(0)} = 0{\cdot}56$ and $\dot{x}_{s_{\mathrm{exp}}}^{(0)} = -0{\cdot}072$.

8. W. LICK, Energy transfer by radiation and conduction, *Proc. 1963 Heat Transfer and Fluid Mech. Inst.*, pp. 14–26, (1963).
9. L. S. WANG, Differential methods for combined radiation and conduction, Ph.D. Thesis in Engineering, Univ. of Calif., Berkeley (1965).
10. L. S. WANG and C. L. TIEN, A study of various limits in radiation heat-transfer problems, *Int. J. Heat Mass Transfer* **10**, 1327–1338 (1967).
11. D. FINKLEMAN, Self consistent solution of nonlinear problems in unsteady radiation gasdynamics, Ph.D. Thesis, M.I.T. (1967).
12. M. C. JISCHKE, Application of the method of parametric differentiation to radiation gasdynamics, Ph.D. Thesis, M.I.T. (1968).
13. K. Y. CHIEN, Radiation dominant interaction in gasdynamics, Ph.D. Thesis, M.I.T. (1968).
14. S. C. TRAUGOTT, Radiative heat flux potential for a nongrey gas, *AIAA Jl* **4**, 541–542 (1966).
15. D. FINKLEMAN and K. Y. CHIEN, Semigrey radiative transfer, *AIAA Jl* **6**, 755–758 (1968).
16. M. A. HEASLET and R. F. WARMING, Theoretical predictions of a radiative transfer in a homogeneous cylindrical medium, *J. Quant. Spectrosc. Radiat. Transfer* **6**, 751–774 (1966).
17. P. CHENG, Two dimensional radiating gas flow by a moment method, *AIAA Jl* **2**, 1662–1664 (1964).
18. C. Y. CHOW, Propagation of self-similar radiation waves, *AIAA Jl* **5**, 2281–2283 (1967).
19. S. C. TRAUGOTT, Shock structure in a radiating, heat conducting and viscous gas, *Physics Fluids* **8**, 834–849 (1965).
20. P. CHENG, Dynamics of a radiating gas with application to flow over a wavy wall, *AIAA Jl* **4**, 238–245 (1966).
21. M. P. SHERMAN, Moment methods in radiative transfer problems, *J. Quant. Spectrosc. Radiat. Transfer* **7**, 89–109 (1967).
22. J. A. MCFADDEN, Initial behaviour of a spherical blast, *J. Appl. Phys.* **23**, 1269–1275 (1952).
23. H. L. BRODE, Numerical solutions of spherical blast waves, *J. Appl. Phys.* **26**, 766–774 (1955).
24. M. P. FRIEDMAN, A simplified analysis of spherical and cylindrical blast waves, *J. Fluid Mech.* **11**, 1–15 (1961).
25. H. A. BETHE, K. FUCHS, J. O. HIRSCHFELDER, J. L. MAGEE, R. E. PEIERLS and J. VON NEUMANN, *Blast Wave*, Los Alamos Sci. Lab. Rept. LA-2000 (1958).
26. J. L. KULANDER, Accuracy of the exponential-kernel approximation to the mean intensity integral, *J. Quant. Spectrosc. Radiat. Transfer* **6**, 527–530 (1966).
27. S. A. RAMSDEN and P. SAVIC, A radiative detonation model for the development of a laser-induced spark in air, *Nature, Lond.* **203**, 1217–1219 (1964).
28. G. A. ASKARYAN, M. S. RABINOVICH, M. M. SAUCHENKO and V. K. STEPANOV, Optical breakdown "fireball" in the focus of a laser beam, *JETP Letters* **5**, 121–124 (1967).
29. R. D. CESS, On the differential approximation in radiative transfer, *ZAMP* **17**, 776–781 (1966).
30. D. B. OLFE, Application of a modified differential approximation to radiative transfer in a gray medium between concentric spheres and cylinders, *J. Quant. Spectrosc. Radiat. Transfer* **8**, 899–907 (1968).
31. Y. S. CHOU and C. L. TIEN, A modified moment method for radiative transfer in nonplanar systems, *J. Quant. Spectrosc. Radiat. Transfer* **8**, 919–933 (1968).
32. S. C. TRAUGOTT, On grey absorption coefficients in radiative transfer, *J. Quant. Spectrosc. Radiat. Transfer* **8**, 971–999 (1968).
33. K. Y. CHIEN, Angular moment averaged absorption coefficients in nongrey radiation, *AIAA Jl* 7, 183–185 (1969).

Résumé—L'interaction entre un champ de rayonnement dominant et un champ d'écoulement est étudée, l'échelle des temps pour une telle interaction instationnaire pouvant être très courte par rapport à un temps "d'écoulement" caractéristique. A l'ordre le moins élevé, il se produit un processus de refroidissement par rayonnement avec un écoulement non couplé, et un développement en nombre de Boltzmann introduit systématiquement des effets d'ordre plus élevé. Un schéma de développement asymptotique raccordé est nécessaire étant donné les longueurs caractéristiques disparates qui existent dans différentes régions spatiales. Les résultats sont présentés dans l'exemple spécifique de l'addition instantanée d'énergie à une région finie avec une symétrie unidimensionnelle (c'est-à-dire, plane, cylindrique et sphérique).

Pour simplifier, le gaz est supposé non visqueux, parafait et en équilibre thermodynamique loçal, et l'approximation différentielle est employée pour le champ de rayonnement. Un schéma numérique a été élaboré pour éviter des itérations qui prennent du temps et les résultats sont comparés à ceux d'une solution analytique restreinte au cas linéaire. Les approximations d'un gas non gris et les effets d'absorption amont sont comprises. Les résultats indiquent un niveau de chauffage amont négligeable, des effets modérés de l'hypothèse d'un gaz non gris, mais des effets importants de la courbure et de l'épaisseur optique. Selon le bilan local entre l'émission et l'absorption, le choc d'explosion peut être soit accéléré soit décéléré. Enfin, on compare l'approximation différentielle et les formulations exactes pour un cas gris plan. L'excellent accord entre le travail actuel et une expérience avec un laser permet de conclure à la possibilité du couplage d'énergie.

Zusammenfassung—Es wird die Wechselwirkung zwischen einem starken Strahlungsfeld und einem Strömungsfeld untersucht, wobei das Zeitmass für solch eine nichtstationäre Wechselwirkung sehr kurz sein möge im Vergleich zu einer charakteristischen Strömungszeit. In erster Näherung ergibt sich ein Kühlungsprozess durch Strahlung mit einer unbeeinflussten Strömung, une eine Ausdehnung auf die Boltzmann-Zahl führt dann systematisch Effekte höherer Ordnung ein. Es wird ein angepasstes asymetrisches Expansionsschema gefordert, angesichts der unterschiedlichen charakteristischen Längen in den verschiedenen Zonen. Dabei werden Ergebnisse angegeben für den speziellen Fall einer plötzlichen Energiezufuhr in einer endlichen Zone mit eindimensionaler Symmetrie (d.h. ebene Zylinder- oder Kugelsymmetrie). Zur Vereinfachung wird das Gas als reibungsfrei, als vollkommen und im thermodynamischen Gleichgewicht angenommen. Es wird weiterhin die differentielle Approximation für das Strahlungsfeld benutzt. Es wird ein numerisches Schema entwickelt, um zeitraubende Iterationen zu vermeiden. Die Ergebnisse wurden verglichen mit jenen aus einer analytischen Lösung, die allerdings auf den linearen Fall beschränkt war. Dabei sind sowohl die nichtgrauen Näherungen als auch die Effekte der Absorption stromaufwärts berücksichtigt. Die Ergebnisse zeigen eine vernachlässigbare Aufheizung stroaufwärts, mässige Effekte des nichtgrauen Gases, aber grosse Auswirkung der Krümmung und der optischen Dicke. In Abhängigkeit vom lokalen Gleichgewicht zwischen Emission und Absorption, kann der Stoss entweder beschleunigt oder verzögert werden. Schliesslich wurde ein Vergleich zwischen der differentiellen Approximation und den exakten Formeln für den ebenen Fall in einem grauen Medium durchgeführt. Die ausgezeichnete Übereinstimmung zwischen der Arbeit und einem Laser-Experiment zeigt, dass auf mögliche Energie-Koppelung geschlossen werden muss.

Аннотация—Исследуется взаимодействие основного лучистого поля с полем потока, когда масштаб времени для нестационарного взаимодействия оченъ мал по сравнению с врменной характеристикой "потока". В первом приближении учитывается лучистое охлаждение отрывного потока, а увеличение числа Больцмана систематически приводит к эффектам высших порядков. Так как характеристические длины различных участков пространства несоизмеримы, требуется специфическая ассимптотическая схема расширения. Приводятся результаты для частного случая мгновенного потока энергии к ограниченной симметричной области (пластина, цилиндр, сфера). Для простоты газ считают невязким, идеальным и находящимся в локальном термодинамическом равновесии; лучистое поле описывается аппроксимированными дифференциальными уравнениями. Во избежание повторений расчета разработана численная схема, а результаты сравниваются с аналитическим решением для линейного случая. В задаче учитывается аппроксимация для несерых газов и эффекты поглощения вверх по потоку. Оказалось, что нагрев вверх по потоку пренебрежимо мал, а наибольшее воздействие оказывают кривизна и оптическая толщина. В зависимости от локального соотношения эмиссии и поглощения, можно ускорить или затормозить ударную волну. В заключении сравнивается принятая аппроксимация с точным решением для случая плоского серого тела. Великолепное соответствие между полученными результатами и экспериментами с лазером позволяет сделать вывод о существовании энергетической связи.